

Breakup of Double Emulsions in Constrictions

Haosheng Chen,^{a,b} Jiang Li,^{c,d} Ho Cheung Shum,^{a,e} Howard A. Stone^c and David A. Weitz^{*a}

Received (in XXX, XXX) Xth XXXXXXXXXX 200X, Accepted Xth XXXXXXXXXX 200X

First published on the web Xth XXXXXXXXXX 200X

DOI: 10.1039/b000000x

We report the controlled breakup of double emulsion droplets as they flow through an orifice of a tapered nozzle. The results are summarized in a phase diagram in terms of the droplet-to-orifice diameter ratio and the capillary number. We identify a flow regime where the inner aqueous phase is released.

Double emulsions, which were originally referred to as emulsion liquid membranes, were conceived for separation and extraction processes¹. With the development of microfluidic multiphase flow technologies, double emulsion have been shown to be an excellent structure for encapsulation and release of active materials in applications such as drug delivery, food processing and cosmetics^{2,3}. Compared with the hydrodynamically controlled breakup of single-phase droplets⁴⁻⁷ in confined geometries, active ingredients have been released by breaking the encapsulating double emulsions thermally^{8,9} or osmotically¹⁰. In some applications, such as drug delivery and oil recovery, the encapsulating structures must go through media with constrictions, such as blood capillaries in the human body or the porous material of a reservoir. In some cases, these constrictions are the locations for release of the active ingredient; thus the double emulsion drops must burst to release its contents. In other cases, the emulsion droplets must be transported through the constrictions to reach the targeted release locations; thus, breakup must not occur in the constrictions. To predict and manipulate the release of actives from such emulsions demands a thorough understanding of the physics of their flow through constrictions, which has not been studied. There have been experimental¹¹ and theoretical studies¹² and simulations¹³ investigating breakup of double emulsions in unbounded shear flows, but the bursting of the inner droplets to escape the double emulsions in confined geometries has not been characterized. Recent advances in microfluidics offer an unique platform to study this important problem. By designing channels with well-defined geometries in microfluidic devices, the flow of double emulsions through controlled constrictions can be investigated experimentally. This study would enable us to predict the behavior of double emulsions in constrictions, and to control the release of the inner phase. In this work, we present a hydrodynamic approach to release actives from the inner phases of double emulsion droplet in a microfluidic device. We first prepare monodisperse double emulsions in capillary microfluidic devices; the resultant double emulsion droplets are reinjected into another capillary device with a tapered channel for studying breakup of the double emulsions. We characterize breakup of double emulsions with a phase diagram based on the capillary number of the flow and the ratio of the droplet-

to-nozzle diameter. The results enable prediction of the breakup of double emulsions.

The generation of double emulsions, and studies of their breakup are performed in two types of microcapillary devices². To make a device for generation of double emulsions, we use pipette puller to taper two cylindrical capillary tubes each with an outer diameter of 1 mm; the resultant capillaries have inner diameters of about 20 μm and 200 μm respectively. The two tapered capillaries are fitted into each end of a square capillary with an inner dimension of 1.05 mm. The innermost phase is water and it flows through the tapered capillary with the smaller tip diameter. The middle phase is polydimethylsiloxane oil containing 2 wt.% surfactant of Dow Corning 749 fluids, which is a blend of approximately 50 percent high molecular weight resin and 50 percent volatile, low viscosity cyclopentasiloxane. The middle phase flows through the interstices between the square capillary and the cylindrical capillary with the small tip. The outer phase is water with 10 wt% polyvinyl alcohol (Sigma-Aldrich), which is a water-soluble synthetic polymer with molecular weight of 13000-23000, and it enters the device through the interstices on the other end. When the three phases meet at the junctions, water-in-oil-in-water (W1/O/W2) droplets form, as shown schematically in Fig. 1(a). The diameters of the inner aqueous phase (W1) and the droplet are controlled by adjusting the flow rates of the different phases. In our experiments, the diameter of the is adjusted approximately from 20 to 150 μm , while the diameter of the double emulsion droplet ranges approximately from 60 to 200 μm .

The double emulsion droplets are collected in a syringe for injection into a second microcapillary device to study droplet breakup. In this second device, only a single round capillary is inserted inside a square capillary tube, and the tapered tip has an inner diameter $d = 10 - 120 \mu\text{m}$ after polishing with sand paper. The double emulsion is injected into the device through the tapered capillary at flow rates $Q = 50 - 15000 \mu\text{l}\cdot\text{h}^{-1}$ while water is injected into the interstices between the round and the square capillary tube at $1000 \mu\text{l}\cdot\text{h}^{-1}$, as shown in Fig. 1b. A high-speed camera (Phantom V7.0) attached to a microscope is used to image the deformation of the double emulsion droplets flowing through the tapered tip. The dynamics of breakup are characterized in terms of the capillary number $Ca = \mu_s U / \gamma_{sc}$, where U is the average velocity of the double emulsion flow at the orifice, μ_s is the viscosity of the middle oil phase (O), and γ_{sc} is the surface tension between the oil phase (O) and inner aqueous phase (W1). For our experiments, $\mu_s = 10 \text{ mPa}\cdot\text{s}$ and $\gamma_{sc} = 31.3 \text{ mN}\cdot\text{m}^{-1}$. In addition, the viscosities of the W1 and W2 are $1 \text{ mPa}\cdot\text{s}$ and $20 \text{ mPa}\cdot\text{s}$,

respectively, and the surface tension of O/W2 is $9.0 \text{ mN}\cdot\text{m}^{-1}$.

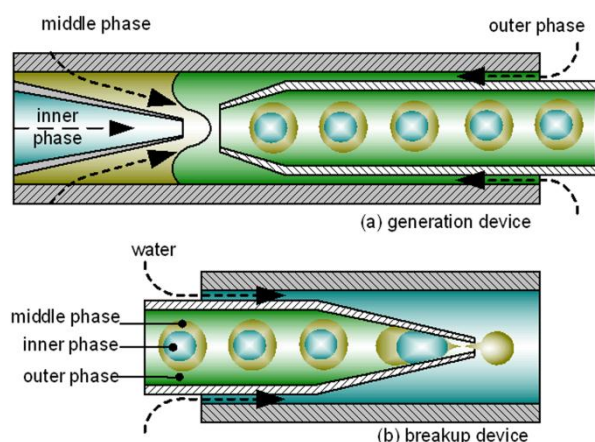


Fig. 1 (a) Schematic of the microfluidic device used for forming double emulsion droplets. (b) Schematic of the device used for breaking up double emulsion droplets, with the droplets flowing from left to right.

To investigate the effect of droplet size on the breakup of double emulsion through constrictions, we inject two double emulsion droplets with different sizes into a capillary with a tapered tip as shown in Fig. 2(a). The small droplet passes through the orifice and retains its O/W2 structure despite large deformations of the droplet at the orifice as shown in Fig. 2(b) and (c). However, for the large droplet, the inner aqueous phase (W1) occupies almost the entire volume of the nozzle, and a neck is formed in the middle oil phase (O) adjacent to the interface with the inner aqueous phase (W1) as shown in Fig. 2(c). Subsequently, the middle oil phase (O) ruptures at the neck and forms two daughter droplets as shown in Fig. 2(d). One daughter droplet is a single-phase oil droplet passing through the orifice, while the other is a W1/O/W2 double emulsion droplet inside the nozzle. As the daughter W1/O/W2 droplet continues its movement through the orifice, the inner droplet of water is released into the continuous phase at the orifice as shown in Fig. 2(e). The remaining oil phase breaks up into two droplets after passing through the orifice as shown in Fig. 2(f). Thus the large double emulsion droplet has completely burst. Our observations suggest that the breakup of double emulsions at narrow constrictions depends on the size of inner aqueous droplets.

To characterize the behavior, we analyze the breakup of a double emulsion droplet as a function of the ratio (D/d) between the diameters of the inner droplets D and the orifice d . We study the behavior of more than 200 double emulsion droplets passing through a tapered capillary and summarize the results in a phase diagram in which the capillary number of the flow is plotted against the ratio of the droplet-to-nozzle diameter. We vary the capillary number mainly through changing the flow velocity, which is easily adjusted in the experiments. However, the capillary number can also be tuned by changing the interfacial tension of the system, as long as the stability of the double emulsion is not compromised. Four types of morphological changes are observed as the double emulsion droplets flow through the nozzle: in the first regime, the entire compound droplet passes through the orifice

without breakup. In the second regime, the inner aqueous phase (W1) is released into the continuous phase. In the third regime, the middle oil phase (O) of the double emulsion droplet breaks up into a smaller double emulsion droplet and a separate oil droplet; the inner aqueous phase (W1) of the double emulsion droplet later bursts into the continuous phase. In the fourth regime, the droplet breaks up into a single droplet and a double emulsion droplet without release of the inner droplet. The fourth regime is rare, and is only observed in less than 2% of the experiments; thus, it is considered to be a transitional state between the first and the third regimes.

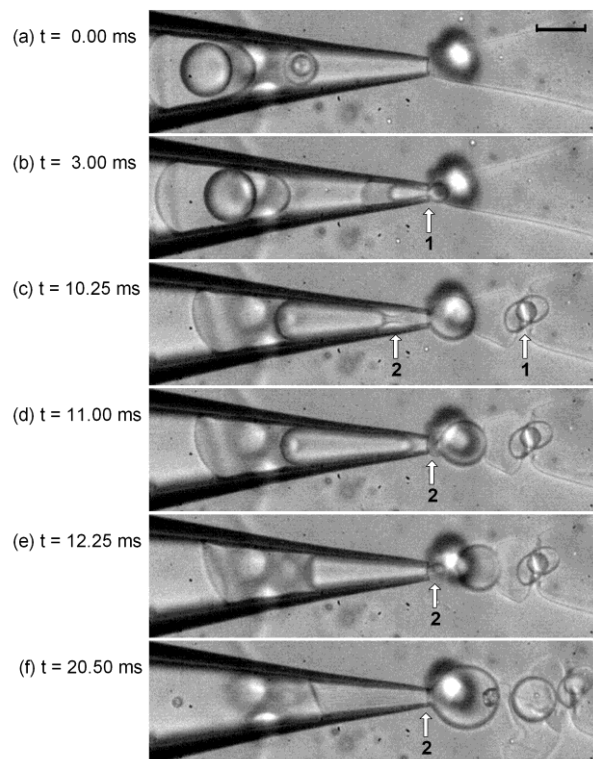


Fig. 2 Behavior of double emulsion droplets of two different sizes flowing through a tapered capillary. Arrows are drawn to indicate the main features of interest. The orifice has an inner diameter of $13 \mu\text{m}$, and the average velocity at the orifice is $U = 2.1 \text{ m/s}$. The scale bar is $50 \mu\text{m}$. (a) Diameters of the inner aqueous phases (W1) of the large and the small droplets are $55 \mu\text{m}$ and $21 \mu\text{m}$, respectively. (b), (c) The small droplet passes through the orifice with deformation in its shape but without breakup, as indicated by arrow 1. (c) The large droplet passes through the orifice, where the middle oil phase (O) forms a droplet; this small daughter droplet is connected to the double emulsion droplet in the capillary through a neck at the tip, as indicated by arrow 2. (d) The neck ruptures and the daughter droplet detaches from the double emulsion droplet at the location indicated by arrow 2. (e) The rest of the middle oil phase (O) ruptures at the orifice, and the inner aqueous phase (W1) is released into the outer aqueous phase (W2), as highlighted by arrow 2. (f) Another daughter droplet is formed. Arrow 2 indicates the same location as in Fig. 2e. A video of this experiment is available in the Supplementary Information.

The behaviors of the droplets at different Ca and with different values of D/d are summarized in Fig. 3. To illustrate how the phase diagram can be used to predict the behavior of the droplets under different conditions, we start with the second regime where the inner aqueous phase (W1) is

released without breakup of the middle oil phase (O), and vary Ca and D/d . When $Ca < 0.1$, the droplets with $D/d > 2$ will have their inner aqueous phase (W1) released into the continuous phase. As D/d becomes larger than 3.8, the middle oil phase (O) will also break up to form two daughter droplets. When $Ca > 0.2$, all the droplets with $D/d \leq 4$ can pass through the orifice without breakup.

The main factor that determines whether double emulsion droplets burst to release the inner droplets is related to the drainage time of fluid in the thin. If this time is shorter than the time for the droplet to flow completely through the orifice, then breakup occurs and the inner aqueous phase (W1) is

released. However, as the flow rate or capillary number is increased, the droplet leaves the orifice in a time too short for the middle oil phase (O) to rupture. This trend is consistent with the transition from regime 2 to regime 1. In this way, the phase diagram enables us to design droplets that break up at specific orifice diameters or at specific flow rates. For droplets with $D/d < 3.8$, increasing the flow rate causes the droplets to pass through the orifice without breakup, while decreasing the flow rate forces the release of the inner droplets into the continuous phase. Alternatively, we can also change the size of the orifice to achieve the desired hydrodynamic response of the droplets.

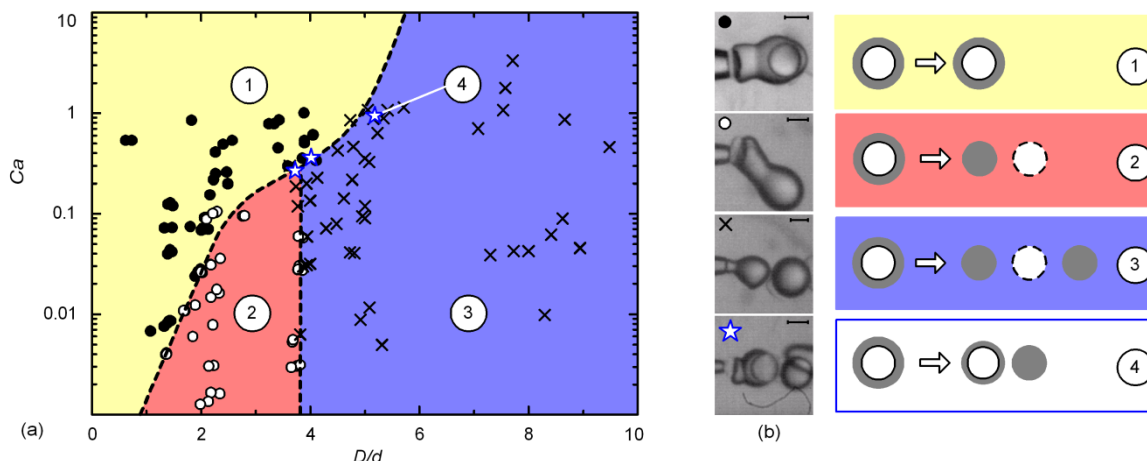


Fig. 3 The behavior of double emulsion droplets at constrictions. (a) A phase diagram of diameter ratio D/d and different capillary numbers Ca . Four different behaviors are observed in the experiments, and the boundary lines between the different regimes are drawn as guides to the eye. Videos of the typical experiments are available in the Supplementary Information. (b) Schematic illustration of the behaviors in the four regimes observed in (a). The images on the right are snapshots observed in each of the four regimes. Scale bars are 100 μm . The sketches on the right illustrate the behavior in the four regimes respectively. The filled gray circles represent the middle oil phase (O), the white circles represent the inner droplet, the black continuous lines represent the interface between the inner aqueous phase (W1) and the middle oil phase (O), and the dashed lines represent the imaginary surface of the inner droplets after release.

In summary, the breakup of double emulsion droplets in constrictions depends on the flow conditions as well as the size of the nozzle. We characterize the behavior in a phase diagram based on the capillary number and the ratio of the diameter of the inner droplets to the size of the constriction. We expect the behavior should be applicable to the coalescence of multiple inner droplets (W1), which should be the same in nature with the coalescence between an droplet (W1) and the continuous phase (W2). This study provides guidelines on sizes of double emulsion droplets needed for release of actives specific to the needs of the applications. The result will enable prediction of the locations at which actives will be released within a complicated network of channels; by applying the concept to the release of chemical reactants, chemical reactions at target positions of a network can potentially be realized.

The authors thank Andrew S. Utada, Yuanjin Zhao, Jeffrey M. Aristoff and other colleagues for helpful conversations. This work was supported by the NSFC (No. 50805008 and No. 50975158), NSF (DMR-1006546), the Harvard MRSEC (DMR-0820484), the Fundamental Research Funds for the Central Universities (FRF-TP-09-013A), and CSC Funding (No. 2009811039 and No. 2009104242).

Notes and references

- ^a School of Engineering and Applied Sciences, Harvard University, Cambridge, MA 02138, USA. E-mail: weitz@physics.harvard.edu
- ^b State Key Laboratory of Tribology, Tsinghua University, Beijing 100084, CHINA.
- ^c Department of Mechanical and Aerospace Engineering, Princeton University, Princeton, NJ 08544, USA. E-mail: hastone@princeton.edu.
- ^d School of Mechanical Engineering, University of Science and Technology Beijing, Beijing 100083, CHINA
- ^e Current address: Department of Mechanical Engineering, University of Hong Kong, Hong Kong, CHINA
- [†] Electronic Supplementary Information (ESI) available: [video for Fig. 2 is shown in Fig2.avi ($Ca = 0.67$, $D/d = 1.6$, $D/d = 4.2$); videos for the four cases in Fig. 3(b) is shown in Fig3_case1.avi ($Ca = 0.26$, $D/d = 2.5$), Fig3_case2.avi (also demonstrate Fig. 4; $Ca = 0.03$, $D/d = 3.7$), Fig3_case3.avi ($Ca = 0.13$, $D/d = 4.0$) and Fig3_case4.avi ($Ca = 0.90$, $D/d = 5.1$), respectively.]. See DOI: 10.1039/b000000x/
- 1 J. Draxler and R. Marr. *Chem. Eng. Process.*, 1986, **20**, 319
- 2 R. K. Shah, H. C. Shum, A. C. Rowat, D. Lee, J. J. Agresti, A. S. Utada, L. Y. Chu, J. W. Kim, A. Fernandez-Nieves, C. J. Martinez and D.A. Weitz, *Mater. Today*, 2008, **11**, 18.
- 3 A. S. Utada, E. Lorenceau, D. R. Link, P. D. Kaplan, H. A. Stone and D. A. Weitz, *Science*, 2005, **308**, 537.
- 4 S. L. Anna, N. Bontoux and H. A. Stone. *Appl. Phys. Lett.*, 2003, **82**, 364.

-
- 5 Y. C. Tan, J. S. Fisher, A. I. Lee, V. Cristini and A. P. Lee, *Lab Chip*,
2004, **4**, 292.
- 6 D. R. Link, S. L. Anna, D. A. Weitz and H. A. Stone, *Phys. Rev.*
Lett., 2004, **92**, 054503.
- 5 7 L. Menetrier-Deremble and P. Tabeling, *Phys. Rev. E*, 2006, **74**,
035303.
- 8 L. Y. Chu, A. S. Utada, R. K. Shah, J. W. Kim and D.A. Weitz,
Angew. Chem. Int. Ed., 2007, **46**, 8970.
- 9 S. Seiffert, J. Thiele, A. R. Abate and D. A. Weitz, *J. Am. Chem.*
10 *Soc.*, 2010, **132**, 6606.
- 10 H. C. Shum, J. W. Kim and D. A. Weitz, *J. Am. Chem. Soc.*, 2008,
130, 9543.
- 11 P. Stroeve and P. P. Varanasi, *J. Colloid Interface Sci.*, 1984, 99, 360.
- 12 H. A. Stone and L. G. Leal, *J. Fluid Mech.*, 1990, **211**, 123.
- 15 13 K. A. Smith, J. M. Ottino and M. O. Cruz, *Phys. Rev. Lett.* 2004, **93**,
204501.